I-B 264

A Nonlinear Finite Element Approach to Analyze Cracking of RC Bridge Piers During Earthquakes

Shiro Takada , Fellow Member; Fac. of Civil Engineering - Kobe University
Freddy Duran C. , Student Member; Fac. of Civil Engineering - Kobe University

Objective

In the study presented herein, assumed mechanisms of concrete-steel interaction and the concrete fracture process are incorporated into an orthotropic plasticity-based damage model in order to prescribe the non-linear post-failure behaviour of concrete under seismic loading including the strain-softening and the stiffness degradation.

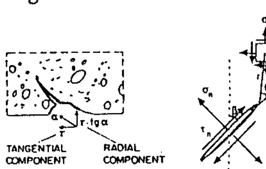

Fig. 1 Acting forces and stresses in concrete within a crack

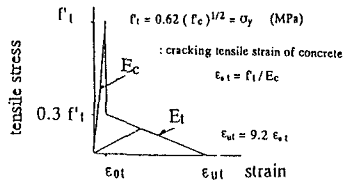

Fig. 2 Stress -strain relationship of concrete in tension considering tension-softening of concrete

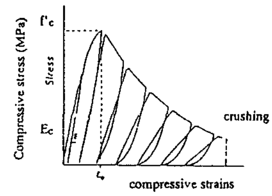

Fig. 3 Uniaxial stress-strain relationship for compression of concrete

The shear stress of the cracked concrete G_{cr} due to sliding friction between crack surfaces represents the only capacity of stress transfer left after a crack is formed (See Fig. 1). G_{cr} can be reduced by using $G_{cr} \doteqdot \beta_s G$, where β_s is the retention factor due to asperities and aggregate interlock. β_s can be assumed to be unity if the crack is closed and 0.5 when the crack is open, The stiffness of the cracked element must be softened isotropically by reducing the elasticity modulus from E_c to E_t according to the assumed in Fig. 2. The tensile stress f_t produced in a crack is integrated along the crack faces in order to obtain equivalent nodal forces at both faces of the crack. The fracture energy G_f is evaluated from the Bazant's relationhip - 1986, as follows:

$$G_f = f_t^2\, h / 2\, E_t \quad \text{(MPa)} \qquad \text{where} \quad h = \sqrt{A}\,, \quad A \text{ is the finite element area} \qquad (1)$$

Crack model

Triangular elements with quadratic shape functions are considered to model the singularity behaviour at the crack tip (See Fig. 4).

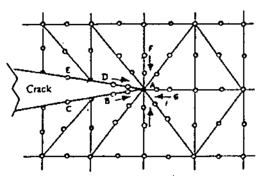

Fig. 4 Finite element model

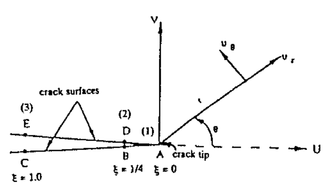

Fig. 5 crack tip discretization

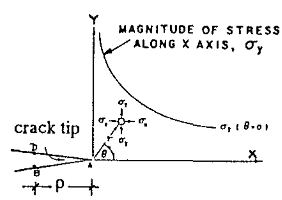

Fig. 6 Stresses representation

The finite element solution can provide the displacements around the crack tip for the combined opening and sliding cracking mechanism (i.e. types I and II, respectively) by considering the following :

$$\begin{bmatrix} \sigma_r \\ \sigma_\theta \\ \tau_{r\theta} \end{bmatrix} = K_I/\sqrt{2\pi r}\,\cos\theta/2 \begin{bmatrix} 1+\sin^2\theta/2 \\ \cos^2\theta/2 \\ \sin\theta/2\cos\theta/2 \end{bmatrix} + (K_{II}/\sqrt{2\pi r}) \begin{bmatrix} (1-3\sin^2\theta/2)\sin\theta/2 \\ -3\sin\theta/2\cos^2\theta/2 \\ (1-3\sin^2\theta/2)\cos\theta/2 \end{bmatrix} \qquad (2)$$

$\sigma_z = \nu'(\sigma_r + \sigma_\theta)$; plane strain $\qquad \sigma_z = \sigma_{rz} = \sigma_{\theta z}$; plane stress

The nodal displacements at nodes B and D can be calculated from Eq. (3) :

$$\begin{bmatrix} u \\ v \end{bmatrix} = [\sqrt{r/2\pi}/(2G/(k+1))] \begin{bmatrix} K_I\,[(2k-1)\cos\theta/2 - \cos 3\theta/2] & + & K_{II}\,[-(2k+1)\sin\theta/2 + \sin 3\theta/2] \\ K_I\,[-(2k-1)\sin\theta/2 + 3\sin 3\theta/2] & & K_{II}\,[(2k-1)\cos\theta/2 - \cos 3\theta/2] \end{bmatrix} \qquad (3)$$

For the combined opening and sliding cracking mechanism the stress intensity factors K_I and K_{II} at element quarter points B and D shown in Fig. 5 are determined by using the following expressions (See Fig. 7):

$$K_I = \sigma_n\sqrt{(\pi/2r)}\,\sin^2\beta \quad \text{kPa-m}^{1/2} \qquad k = 3-4\nu \quad \text{plane strain}$$

$$K_{II} = \sigma_t\sqrt{(\pi/2r)}\,\sin\beta\,\cos\beta \quad \text{kPa-m}^{1/2} \qquad k = (3-\nu)/(1+\nu) \quad \text{plane stress} \qquad (4)$$

Cracking of concrete in Finite Element Analysis

The concrete is considered isotropic before cracking. When the cracking is initiated due to excessive tension in the axis normal to cracks the concrete becomes orthotropic, this stage is characterized by Eq. (5) :

$$\begin{bmatrix} \sigma_n \\ \sigma_t \\ \tau_{nt} \end{bmatrix} = \begin{bmatrix} E_n & \nu & 0 \\ \nu & E_t & 0 \\ 0 & 0 & \beta_s G \end{bmatrix} \begin{bmatrix} \varepsilon_n \\ \varepsilon_t \\ \gamma_{nt} \end{bmatrix} \quad (5)$$

Because the tensile cracking has occurred previously in a plane defined by the normal **n** , the biaxial condition $\sigma_n - \tau_n$ described by Eq. (6) is considered herein.

$$F(\sigma, \varepsilon_{np}) = \sigma_n^2 + \tau_{nt}^2/\alpha^2 - f_t^2 = 0 \quad (6)$$

Then, the post-cracking stage is governed by :

$$\begin{bmatrix} \sigma_n \\ \sigma_t \\ \tau_{nt} \end{bmatrix} = \begin{bmatrix} E_{11}(1 - 4E_{11} c\sigma_n^2) & 0 & -4cE_{11} G \sigma_n \tau_{nt}/\alpha^2 \\ 0 & E_{11} & 0 \\ & & G(1 - 4c\, G\tau^2_{nt}/\alpha^4) \end{bmatrix} \begin{bmatrix} \varepsilon_n \\ \varepsilon_t \\ \gamma_{nt} \end{bmatrix} \quad (7)$$

where : $c = 1/(E_p + 4\sigma_n^2 E_n + 4\tau_{nt}^2 G/\alpha^4)$; $E_{11} = E/(1 - \nu^2)$

$E_p = 4 f_t \sigma_n E_n h$ = plastic strain-softening modulus

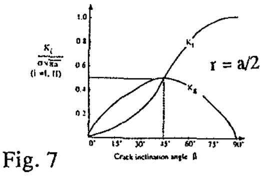

Fig. 7 K_i vs crack inclination β for a crack in tension

Model problem

A single RC bridge pier supporting a typical steel girder (See Fig. 8) is analized herein. The motion considered is a piece-linear wave of 4 sec. of duration and 0.4g of max. acceleration.The time step is 0.05 sec.

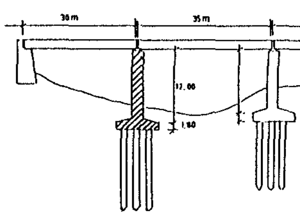

a) Bridge model

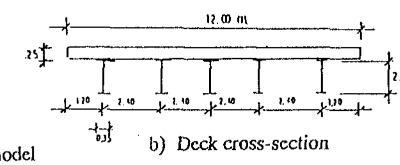

b) Deck cross-section

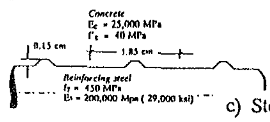

c) Steel reinforcing bar

Fig. 8 Geometric characteristics of the bridge pier

Numerical results

Fig. 9 shows the variation of cracking moment M_{cr} along the height of the pier. The change in the slope indicates the sensivity to cracking from approximately the midheight of the pier (at which lap-splices are considered) to the top.
This slope is expected to decrease up to small values of moments in case of slender columns.
Cracking of concrete at the bottom of piers are produced by relative large moments. Finally, this figure also indicates the need of strong confinement from the lap-splice zone to the bottom of the pier.

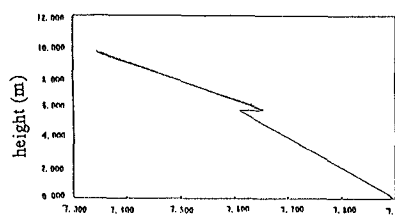

Fig. 9 Cracking rotations along the height of the pier

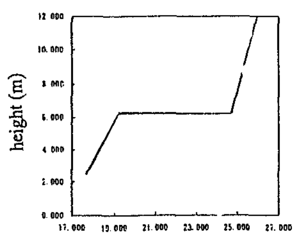

Fig. 10 Ultimate displacements versus height of the pier

Fig. 10 shows the variation of ultimate displacements along the height of the pier. The brusque change at approximately the midheight of the pier implies a large rotation and deformation at the midheight. This effect is physically reflected in the extensive concrete cracking and twisting of steel reinforcement. The large displacement implies a very significative degradation in the shear capacity at this section. Under this conditions the effective cross section is strongly reduced exposing reinforcing bars which without proper confinement will buckle first, and pulled-out after, producing the collapse of this pier.

Conclusions

Cracking of RC bridge piers under cyclic loading can be represented by the combination of both the nonlinear finite element theory and the mixed-fracture mode of fracture mechanics theory. The adopted concrete tensile stress law is considered to be decisive in the cracking stage. Finally, results shows reasonable agreement if they are compared with seismic response of similar structures obtained by other researchers.